GEOPHYSICAL RESEARCH LETTERS, VOL. 23, NO. 17, PAGES 2275-2278, AUGUST 15, 1996

Seafloor Magnetotelluric Sounding Above Axial Seamount

Graham Heinson
School of Earth Sciences, Flinders University, Bedford Park, Australia

Steven Constable
Institute of Geophysics and Planetary Physics, University of California San Diego, La Jolla

Antony White
School of Earth Sciences, Flinders University, Bedford Park, Australia

Abstract. Axial Seamount is a large, active, ridge axis volcano located on the central segment of the Juan de Fuca Ridge in the northeast Pacific Ocean. Magnetotelluric (MT) data have been collected at three sites, approximately 4 km apart around the eastern rim of the volcano, during a 65-day deployment. MT responses, in the bandwidth of 10^2 – 10^5 s, are almost isotropic, with a weakly-defined principal direction of strike parallel to the main topographic trends of Axial Seamount, and are relatively flat over the whole bandwidth. Apparent resistivities are of the order of 7 – 20 Ωm, and phases are as low as 30° at the short periods. Diagonal terms of the MT tensor are an order of magnitude smaller than the off-diagonal terms, suggesting that three-dimensional effects on the data are minimal. Two-dimensional inversions suggest that seafloor bathymetry and the distant coastlines have a surprisingly small effect on the MT response, and one-dimensional inversions fit the MT data to within the errors with no serial correlation in the residuals. A low crustal resistivity is the most robust part of the model, probably due to seawater in fractures and possibly due to a magma chamber. An electrical asthenosphere, although less well constrained, exists over a depth range 30 – 60 km, and the resistivity of this region is compatible with about 8% fraction of melt.

Introduction

Axial Seamount lies on the intersection of the Cobb-Eickelberg Seamount Chain and the Juan de Fuca Ridge, about 500 km west of the Oregon (USA) coast. The volcano (Plate 1) is the shallowest part of the Juan de Fuca Ridge, indicating a significant and robust supply of magma [e.g. *Delaney et al.*, 1981], and is currently volcanically and hydrothermally active, with evidence of recent lava flows, hydrothermal activity, and deformation [*Embley et al.*, 1990; *Fox*, 1990]. Foward modeling and inversion of sea-surface magnetic anomaly data [*Tivey and Johnson*, 1990] indicates a temperatures of greater than 200°C at a depth of 700 m beneath the caldera, suggesting the presence of a magma chamber at 3 km depth below the summit, or a zone of extensive subsurface alteration. *Hildebrand et al.* [1990] model sea-surface gravity anomalies and seafloor gravity measurements to infer the existence of a shallow, low-density region. The low-density region could be melt, but other factors, such as porosity and mineralogy, are important.

Paper number 96GL01673
0094-8534/96/96GL-01673$05.00

Instrumentation and Data

Three sets of magnetotelluric (MT) instruments were deployed from 3rd July to the 7th September, 1994. The GPS-determined deployment locations and depths (Plate 1) were for Pele 45° 55.47' N, 129° 59.03' W (1550 m), Macques 45° 57.48' N, 129° 58.98' W (1520 m) and Ulysses 45° 59.50' N, 129° 59.81' W (1490 m).

Electric fields were recorded by the two-component short-armed electrometer described in *Constable and Cox* [1996], with the high-gain AC amplifiers replaced by lower gain DC amplifiers. The least-count was 0.006 μV and the sample rate 1 s. The magnetometers, developed at Flinders University [*White*, 1979], are installed in standard 17 inch glass instrument housings, which were swapped with one of two glass buoyancy floats in the E-field package. The three-component ring-core fluxgate sensors had a least-count of 0.1 nT and a sample rate set at 30 s. Additionally, a two-axis clinometer recorded the magnetometer tilt with a precision of 0.01° every 78 minutes during the deployment.

Three complete 65 day records were obtained from the electrometers. Electrode potential drifts were rapid over the first 5 to 10 days, of the order of 20 μV/day, but steadied to a relatively monotonic variation of less than 5 μV/day for the remainder of the experiment. The magnetometer records ranged from 65 days at Pele, 10 days at Macques and 4 days at Ulysses. Tilt records indicated angles of magnetometer repose of the order of 1 – 5° in both x and y–orientations. Some ocean tidal variations of the order of 0.2° were present in the Ulysses tilt records, but Macques and Pele showed little or no movement.

For each site, time series data were processed to obtain MT responses using the methods and computer code of *Egbert and Booker* [1986]. Data from the Victoria Magnetic Observatory were used as a remote reference. Without the remote reference, uncorrelated noise in the horizontal magnetic field data reduces the MT impedance, so that the apparent resistivity drops off rapidly with the power spectra of the electric field, although phases are less affected. MT response estimates were obtained for sites Macques and Pele. The short duration of the Ulysses magnetometer record resulted in much poorer responses which have not been used.

MT responses were obtained in the bandwidth 2×10^2 to 6×10^4 s; at shorter periods coherences dropped rapidly and at longer periods source-field effects became dominant [*Wannamaker et al.*, 1989a]. The MT impedance tensor was then rotated to find the dominant strike by the decomposition method of *Lilley* [1995]. Rotation angles were approximately frequency independent, and gave a predominant strike of about 20° and 30° west of geomagnetic north for Pele and Macques

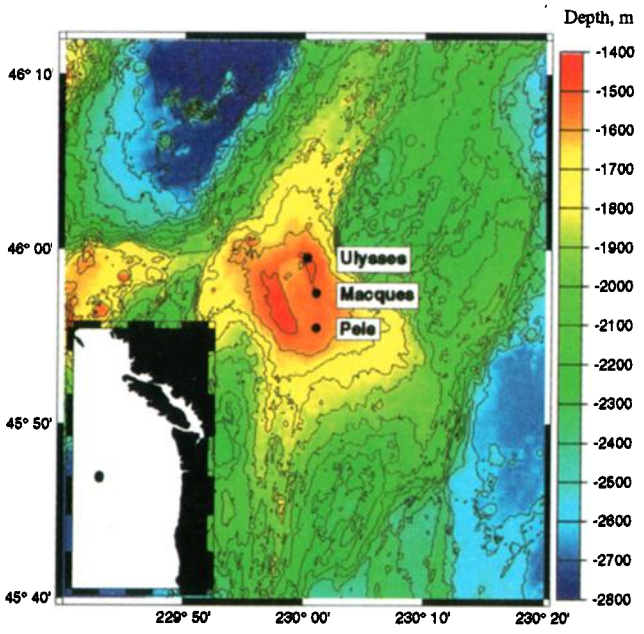

Plate 1. Site location of Axial Seamount and the three deployed MT instruments

respectively. These orientations are most sensitive to local seafloor bathymetry changes and the trend of the coastline.

Figure 1 shows the MT responses, with error estimates, at Pele. The most notable features of these plots are that the MT data are almost isotropic, and apparent resistivities are low, of order 10 Ωm. Differences in the along-axis MT responses (TE mode) at Macques and Pele are generally within the error estimates. Across-axis (TM mode) apparent resistivities are slightly larger at Macques, but phases are similar. Diagonal elements of the MT tensors at both sites have apparent resistivities which are an order of magnitude smaller than the off-diagonal elements, from which we conclude that 3D effects on the data are minor.

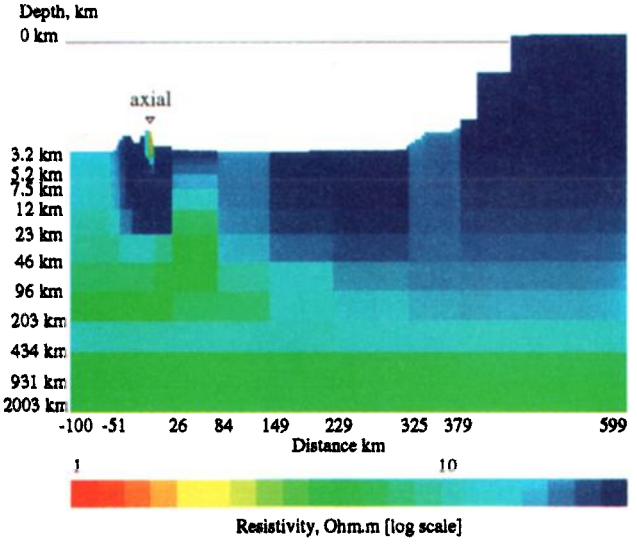

Plate 2. 2D smooth Occam's inversion of both Pele TE and TM modes for a transect passing through the coastline and Axial Seamount. The transect has a strike direction of 90° east of geographic north. The RMS misfit is 1.0.

MT Response Interpretation

Heinson and Constable [1992] argued that for an electrically resistive oceanic lithosphere underlying the whole ocean basin, seafloor MT data will be significantly distorted from 1D due to the coast-effect. *Tarits et al.* [1993] pointed out that in the presence of leakage paths to more conductive parts of the mantle, the coast-effect distortion was much reduced, and suggested that subduction zones may represent such a leakage path, as was thought to be the case in the EMSLAB experiment [*Wannamaker et al.*, 1989b]. Here we make the case that Axial Seamount may also act as a leakage path to the asthenosphere.

The evidence for a low resistivity path to the mantle is threefold. Firstly, the observed isotropic MT response would not be predicted from the coast-effect alone. Although *Heinson and Constable* [1992] showed that isotropic MT responses may occur in an ocean basin with no leakage paths to the deep mantle, it required the site to be approximately equidistant to two or more orthogonal coasts. For Axial Seamount, this is not the case as it is much closer to the coastline of western North America (450 km) than any other coast. Secondly, apparent resistivities in the TE orientation are smaller than similar seafloor MT responses on the Juan de Fuca Plate [*Wannamaker et al.*, 1989a] and elsewhere. Finally, we note that relatively flat MT response over two decades of period suggests that the resistivity structure beneath Axial Seamount is relatively uniform with depth. To test these hypotheses, we have inverted the data using 1D and 2D techniques.

A 2D inversion, using the Occam's algorithm of *deGroot-Hedlin and Constable* [1990], was used to examine the effect of ridge topography and the North American coastline. A profile was chosen perpendicular to the coast which passed through sites of Macques and Pele. Inverting single-site MT responses for 2D structure may seem somewhat ambitious. However, bathymetry and coastlines, coupled with seawater resistivity, provides additional constraints on the modeling.

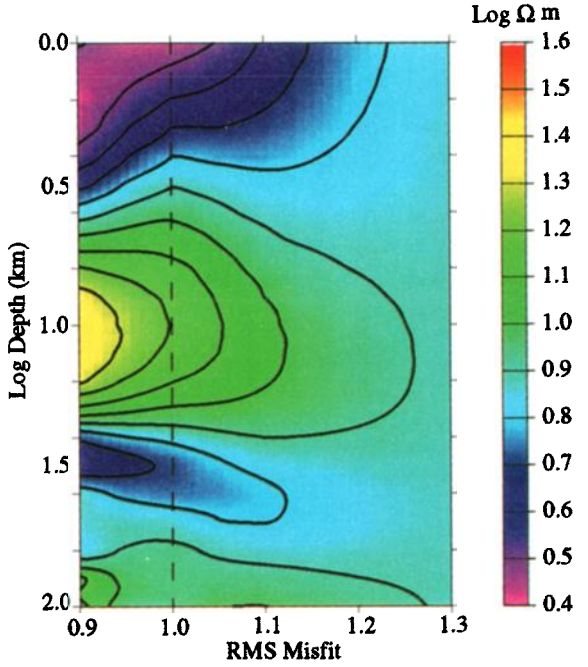

Plate 3. 1D Occam inversions, with first derivative roughness, of the TE responses at site Pele for RMS values varying from 0.9 to 1.3. The dashed line shows the preferred misfit level, the profile is shown in Figure 2.

Although there are many more model parameters than data, parts of the model that are unresolved are simply determined by the smoothing penalty.

The 2D inversion of Pele MT data is shown in Plate 2, and gives a fit to the TE and TM responses to within the error estimates (RMS = 1.0) with no serial correlation of residuals. The fit to Macques MT data is marginally worse (RMS = 1.7), but the final model is essentially the same as for Pele. The resistivity structure directly beneath Axial Seamount is constrained primarily by the TE component, and we find that seafloor topography is sufficient to generate the observed difference between the TE and TM modes for both sites.

To examine the resistivity structure beneath Axial Seamount more fully, the TE responses were inverted for 1D structure using the D^+ algorithm [*Parker and Whaler*, 1981]. The utility of the D^+ algorithm is that it gives the minimum possible RMS misfit and therefore can be used to test whether data are compatible with a 1D structure. For Pele, the RMS misfit to the TE data was 0.8, and for Macques the RMS misfit was 1.0. In both cases, no significant trends of serial correlation in the model residuals were present. Such model fits suggest that these MT responses are compatible with 1D structure.

Smooth resistivity models, using the 1D Occam's algorithm [*Constable et al.*, 1987], which fits the TE response at Pele to an RMS misfits of 1.0 is shown in Figure 2. Here we show profiles when penalising both the first and second derivative of the roughness. The coincidence of of the two models supports the interpretation over the depth range shown. 1D inversion of Macques TE data produces similar structure. The most striking features in Figure 2 are the low resistivity in the crust and the drop in resistivity over depths of 30 – 60 km. To examine the resolution of the inversion, we show, in Plate 3, inversions for different levels of RMS misit, ranging from RMS = 0.9 which is the smallest obtainable, to RMS = 1.3 at which all structure disappears. Plate 3 clearly shows that the most persistent part of the profile is the low resistivity at shallow depths, which is still identifiable to RMS = 1.2. However, the mid-mantle fall in resistivity is less well constrained by the data.

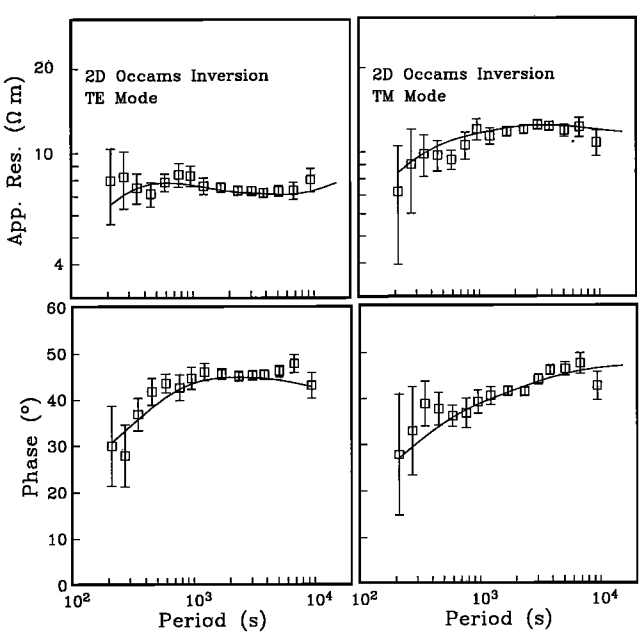

Figure 1. Observed Pele TE and TM mode MT responses with error estimates, and the modeled responses (solid lines) from the 2D section shown in Plate 2. The RMS misfit is 1.0.

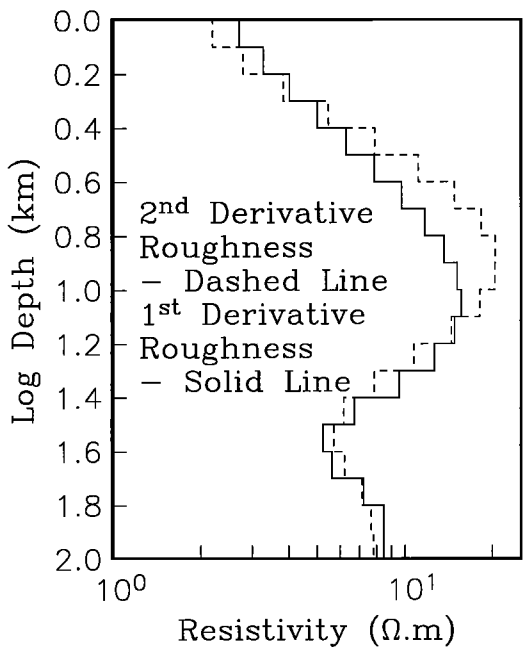

Figure 2. 1D Occam inversions of the TE responses at site Pele. The solid line shows the first derivative roughness and the dashed line shows the second derivative roughness. The RMS misfits are 1.0 for both inversions.

Tectonic Interpretation

The models in Figure 2 suggest that the electrical resistivity of the crust beneath the summit of Axial Seamount is anomalously low, approaching 1 Ωm. Although we have little resolution of the crust, as skin depths at the shortest periods will be at least 5 km, the MT responses are sensitive to crustal structures. Absolute resistivities cannot be determined, however the crustal conductance (defined as the depth-integrated conductivity) is relaively robust to the RMS misfit in Plate 3, and can be estimated to be of order 1,000 S. This is considerably higher than expected for oceanic crust away from a ridge or seamount. For example, the in situ measurements of *Becker et al.* [1982] over the top 2 km, suggest a crustal conductance to be at about an order of magnitude smaller.

The mechanism producing high crustal conductance is most probably due to a fluid fraction, either seawater in fractures and/or molten rock in a magma chamber. Assuming a fully interconnected fluid fraction, which is equivalent to using Archies' Law with an exponent of 1.2 [*Evans*, 1994], and fluid conductivity of 0.31 Ωm, the conductance of a 6 km thick crust requires a bulk porosity of 9 %. This is not unreasonable for hydrothermal fluids in highly fractured basalt over the top few hundreds of metres. The electrical resistivity of the hydrothermal fluids also decreases with temperature. The presence of additional melt can neither be excluded or supported as the thermal structure and porosity of Axial Seamount are unknown.

An increase in resistivity below the crust to 20 Ωm at 10 – 30 km depth is an important feature if it can be constrained by the data. Such a rise in resistivity suggests that significant melt fractions do not connect with a deeper mantle melting source. From geochemical and petrological arguments, only a small amount of melting is expected in the plagioclase peridotite stability field at depths less than 20 km below the seafloor [*Elthon*, 1989]. High temperatures at or slightly below the

mantle geotherm of approximately 1280°C will give rise to resistivities of the order of 50 Ωm [*Constable et al.*, 1992]. We lack the data quality and spatial distribution to constrain this layer more precisely.

The model in Figure 2 has a fall in resistivity over a depth interval of 30 – 60 km in the mantle, which is weakly constrained by the MT responses. A resistivity of the order of 5 – 10 Ωm suggests high temperatures and possibly a small melt fraction. Geochemical and petrological studies roughly constrain the depths where most basaltic melt is generated. Small amounts of melting occurs in the garnet lherzolite stability field (65 – 80 km depth), but most melting occurs in the spinel peridotite stability field (20 – 65 km) [e.g. *Elthon*, 1989]. MORB geochemical and petrological studies suggest that an average of 10 – 15% of the sub-ridge mantle melts, with a maximum melt extraction of 20 – 30%. Some authors [e.g. *Sotin and Parmentier*, 1989] suggest that the melt is rapidly drained from the mantle and less than 3% is present at any time. Assuming a maximum melt percentage of 30%, and using Archies' Law with an exponent of 1.2, the resistivity could approach 1 Ωm, but for 3% melt the corresponding resistivity is 20 Ωm. An 8% melt fraction gives resistivities of 15 Ωm, compatible with the 1D inversions.

Conclusions

Seafloor MT data collected on the summit of Axial Seamount suggest that the electrical resisitivity of the crust is low, and that there is an additional low resistivity layer at 30 – 60 km depth. Electric currents induced in the sea are therefore able to leak into the conductive parts of the mantle. Supporting evidence for this comes from almost isotropic MT responses with minimal 2D or 3D effects in spite of the close proximity of the coastline. The MT data are fit to the observed errors by 1D inversion, and bulk properties, such as the percentage of either melt or hydrothermal fluids, can be estimated from inverted resistivities. Average crustal porosity in the upper 6 km is about 9%, and over a depth range of 30 – 60 km resistivities may be associated with a melt fraction of 8%.

Acknowledgments. We thank the captain and crew of the R/V Wecoma. Tom Deaton, Jacques Lemire, Brenton Perkins and Bob Walker provided technical support, and financial support came from the Australian Research Council, the National Science Foundation, and a Japan Society for the Promotion of Science Fellowship. The Canadian Geological Survey kindly supplied magnetic observatory data.

References

Becker, K., et al., In situ electrical resistivity and bulk porosity of the oceanic crust, Costa Rica Rift, *Nature*, **300**, 594-598, 1982.

Constable, S.C., R.L. Parker and C.G. Constable, Occam's inversion: a practical algorithm for generating smooth models from electromagnetic sounding data, *Geophysics*, **52**, 289-300, 1987.

Constable, S., Shankland, T.J. and Duba, A., The electrical conductivity of an isotropic olivine mantle, *J. Geophys. Res.*, **97**, 3,397-3,404, 1992.

Constable, S., and C.S. Cox, Marine controlled-source electromagnetic sounding 2. The PEGASUS experiment, *J. Geophys. Res.*, **101**, 5519-5530, 1996.

deGroot-Hedlin, C. and S. Constable, Occam's inversion to generate smooth, two-dimensional models from magnetotelluric data, *Geophysics*, **55**, 1,613-1,624, 1990.

Delaney, J.R., H.P. Johnson, and J.L. Karsten, The Juan de Fuca Ridge-hot spot-propagating rift system: New tectonic, geochemical and magnetic data, *J. Geophys. Res.*, **86**, 11,747–11,750, 1981.

Egbert, G.D. and J.R. Booker, Robust estimation of geomagnetic transfer functions, *Geophys. J. R. Astr. Soc.*, **87**, 173-194, 1981.

Embley, R.W., K.M. Murphy and C.G. Fox, High-resolution studies of the summit of Axial Volcano, *J. Geophys. Res.*, **95**, 12,813-12,822, 1990.

Elthon, D., Pressure of origin of primary mid-ocean ridge basalts, in *Magmatism in the Ocean Basins*, edited by A.D. Saunders and M.J. Norry, Geological Soc. Spec. Pub., pp. 125-136, 1989.

Evans, R.L., Constraints on the large-scale porosity and permeability structure of young ocean crust from velocity and resistivity data, *Geophys. J. Int.*, **119**, 869-879, 1994.

Fox, C.G., Evidence of active ground deformation on the mid-ocean ridge: Axial Seamount, Juan de Fuca Ridge, April-June 1988, *J. Geophys. Res.*, **95**, 12,813-12,822, 1990.

Heinson, G., and S. Constable, The electrical conductivity of the oceanic upper mantle, *Geophys. J. Int.*, **110**, 159-179, 1992.

Hildebrand, J.A., J.M. Stevenson, P.T.C. Hammer, M.A. Zumberge, R.L. Parker, C.G. Fox and P.J. Meis, A seafloor and sea surface gravity survey of Axial Volcano, *J. Geophys. Res.*, **95**, 12,751-12,763, 1990.

Lilley, F.E.M., Strike direction: obtained from basic models for 3D magnetotelluric data, in *Three-dimensional electromagnetics*, editors M. Oristaglio and B. Spies, Schlumberger-Doll Research, Ridgefield, Conn., USA,pp 359-369, 1995.

Parker, R.L. and K.A. Whaler, Numerical methods for establishing solutions to the inverse problem of electromagnetic induction, *J. Geophys. Res.*, **86**, 9,574-9,584, 1981.

Sotin, C. and E.M. Parmentier, Dynamical consequences of compositional and thermal density stratification beneath spreading centres, *Geophys. Res. Lett.*, **16**, 835-838, 1989.

Tarits, P., Chave, A.D. and Schultz, A., Comment on 'The electrical conductivity of the oceanic upper mantle' by G. Heinson and S. Constable, *Geophys. J. Int.*, **114**, 711-716, 1993.

Tivey, M.A. and H.P. Johnson, The magnetic structure of Axial Seamount, Juan de Fuca Ridge, *J. Geophys. Res.*, **95**, 12,735-12,750, 1990.

Wannamaker, P.E., et al., Magnetotelluric observations across the Juan de Fuca subduction system in the EMSLAB project, *J. Geophys. Res.*, **94**, 14,111-14,125, 1989a.

Wannamaker, P.E., J.R. Booker, A.G. Jones, A.D. Chave, J.H. Filloux, H.S. Waff and L.K. Law, Resistivity cross section through the Juan de Fuca ridge subduction system and its tectonic implications *J. Geophys. Res.*, **94**, 14,127-14,144, 1989b.

White, A., A seafloor magnetometer for the continental shelf, *Mar. Geophys. Res.*, **4**, 105-114, 1979.

Graham Heinson, School of Earth Sciences, Flinders University, Bedford Park, SA 5042, Australia. (e-mail: graham.heinson@flinders.edu.au)

Steven Constable, University of California San Diego, Scripps Institution of Oceanography, Institute of Geophysics and Planetary Physics 0225, La Jolla, CA 92093-0225. (e-mail: sconstable@ucsd.edu)

Antony White, School of Earth Sciences, Flinders University, Bedford Park, SA 5042, Australia. (e-mail: mgaw@es.flinders.edu.au)

(Received January 31, 1996; revised March 29, 1996; accepted May 17, 1996.)